Experiments in Fluids 16, 73–81 (1993)

Experiments in Fluids

Bluff-body drag reduction by passive ventilation

G. K. Suryanarayana[1], Henning Pauer[2], G. E. A. Meier[2]

[1] Experimental Aerodynamics Division, National Aerospace Laboratory, Bangalore, India
[2] DLR Institute for Experimental Fluid Mechanics, Goettingen, Germany

Received: 4 March 1993 / Accepted: 9 March 1993

Abstract. The drag of a sphere at high *Re* can be reduced to more than half its value by passive ventilation from the stagnation region to the base. Simultaneously, the flow field around the base is stabilized and made symmetric, leading to reduction of unsteady aerodynamic forces. At high *Re*, the vent flow breaks through the dead water region associated with the near wake and aerodynamically streamlines the base. The streamlining is done by virtue of a base-vortex-ring beyond the point of turbulent boundary layer separation. A mean flow model for the flow around the vented sphere is proposed.

Smoke flow visualized on a laser light screen placed at two diameters behind the base of the sphere shows the effectiveness of the method in suppressing the flow oscillations.

The drag reduction achieved is very sensitive to the quality of the external surface and relatively insensitive to disturbances in the internal flow. Surface roughness or boundary layer tripping wire on the external flow can completely offset the benefit obtained.

1 Introduction

It is well known that pressure drag due to flow separation constitutes more than 90% of the total drag of bluff bodies (Aachenbach 1972). Delaying the separation by streamlining or by employing vortex generators to sweep away the retarded boundary layer flow using the potential flow are some of the known methods of drag reduction (Lin et al. 1990, Gad-el-Hak and Bushnell 1991).

The splitter plate experiments of Roshko (1954) on two-dimensional bluff-bodies show that the suppression of periodic vortex shedding leads to base pressure increase and a consequent drag reduction. Wood (1964) and Bearman (1967) have studied the effect of bleeding a secondary stream of air into the wake of a blunt based airfoil. It is reported that base bleed causes the base pressure to increase up to a certain limit and then the effect is negative. Base bleed is said to delay the onset of instabilities in the shear layer and thus cause a delay in the position of the roll-up of the shear layers, which causes the base pressure increase. The effect is greater when the area of the jet is large as compared with that of the base. However, base bleed is unlikely to be a practical method for drag reduction considering the device drag (Mair 1978).

The present concept of ventilation is described in detail by Meier et al. (1990). Flow field around a bluff-body causes a stagnation region around the front and a low pressure region surrounding the rear. When these two regions are interconnected or ventilated by an internal duct through the center of the body, an internal flow driven by an effective pressure gradient is set up automatically by the external flow. Consequently, additional mass, momentum and energy are added in the near wake. The vent flow emerging from the base and the external shear layer have opposing vorticities and a constructive interaction between them can lead to base pressure increase and a corresponding drag decrease.

The concept of ventilation is notably different from that of base bleed. In the case of venting, the mass flow ejected into the wake is determined entirely by the external pressure distribution and the base pressure is changed. The modified base pressure affects the external pressure distribution. Thus, a fluid dynamic feed-back is caused. In base bleed, the secondary flow is an independent flow, governed by the energy input.

It appears that very few results based on the concept of ventilation on bluff bodies have been reported. According to Wong (1985), small amounts of base bleed can stop vortex induced oscillations of a circular cylinder at *Re* of 1800 and 2790 from tests in a water tunnel. In these tests, ventilation was effected at two locations symmetrical about the centerline on the base of a cylinder model from the stagnation region by using a concentric inner cylinder. It is reported that a central vent has a greater stabilizing effect than venting at other locations in the base. In this experiment, the internal flow undergoes large pressure losses which might be crucial for the efficiency of the method.

Correspondence to: G. K. Suryanarayana

In a recent study, Meier et al. (1990) have reported a 10% drag reduction obtained by venting spheres at a subcritical *Re*. It is further reported that in the case of a vented cylinder, the effect in the near wake is greatest when the internal duct has a divergence.

In this paper, we present results from experiments on centrally vented spheres. Drag measurements and flow visualizations will be discussed and a possible mean-flow model is proposed. Some of the results were reported by Suryanarayana et al. (1992). The work reported forms a part of the doctoral thesis of the first author.

2 Description of the models and the experimental set-up

2.1 Water tunnel experiments

Solid wooden spheres of 39 mm and 79 ram diameters were drilled along a diameter to obtain 6 mm and 12 mm diameter holes respectively. This provides a vented area of 2.25% of the projected area of the sphere. A water resistant paint was applied on the surface to obtain a smooth finish. 6 mm and 12 mm diameter stings were fixed at about 90° positions from the centerline respectively on the two spheres. The experiments were carried out in a water tunnel of test section size 250 x 330 mm resulting in blockage ratios of 1.5% and 5.9% respectively. The test *Re* was varied from 1700 to 21500.

Flow visualizations were performed using hydrogen bubble technique and dye-flow techniques. The dye used was a mixture of uranine dye and food colours. The visualizations were recorded on a video tape.

2.2 Wind tunnel experiments

The models were made from commercially available styrofoam spheres of 200 mm diameter. Three venting configurations were chosen. All the three had 30 mm vent hole in the front. At the rear, the diameters were chosen to be 20 mm, 30 mm and 50 mm, so that the configurations provide a 3° convergence, a parallel flow and a 6° divergence respectively. Fig. 1 shows a photograph of the model and the support system in the open jet test section of the 1 m tunnel at DLR. The wind tunnel has a closed circuit and provides a free jet from a nozzle with rectangular exit of dimensions 1 m x 0.75 m. The maximum free stream velocity is 55 m/s which corresponds to $Re = 8.5 \times 10^5$ for the sphere. The free stream turbulence intensity is 0.15%.

Axial force on the model was measured using a single component strain gauge balance manufactured by Hottinger-Baldwin Messtechnik (HOTTINGER BALDWIN MEßTECHNIK Gmbh, Postfach 4235, Im Tiefensee 45, 64293 Darmstadt I, Germany) and has a range of 50 N. Drag due to the support system alone was measured by supporting the model from an alternate position in which the effect of the wake of the model on the support system was identically simulated, Identical corrections were applied for all the spheres.

For all the force measurements, the force data was averaged over 2()s. Free stream velocity was measured by measuring the pressure differencebetween the atmosphere and the settling chamber using a Setra differential pressure transducer of range 13 mBar. The data were digitized and acquired on a PDP computer. Oil-flow visualizations were performed using a mixture of Fiesta fluotracer dissolved in petroleum. Smoke flow visualizations were performed using a Disco smoke generator placed in the settling chamber. Laser light sheet was produced in the test section at several planes normal to the flow and also along the flow using a cylindrical lens attached to a 5W

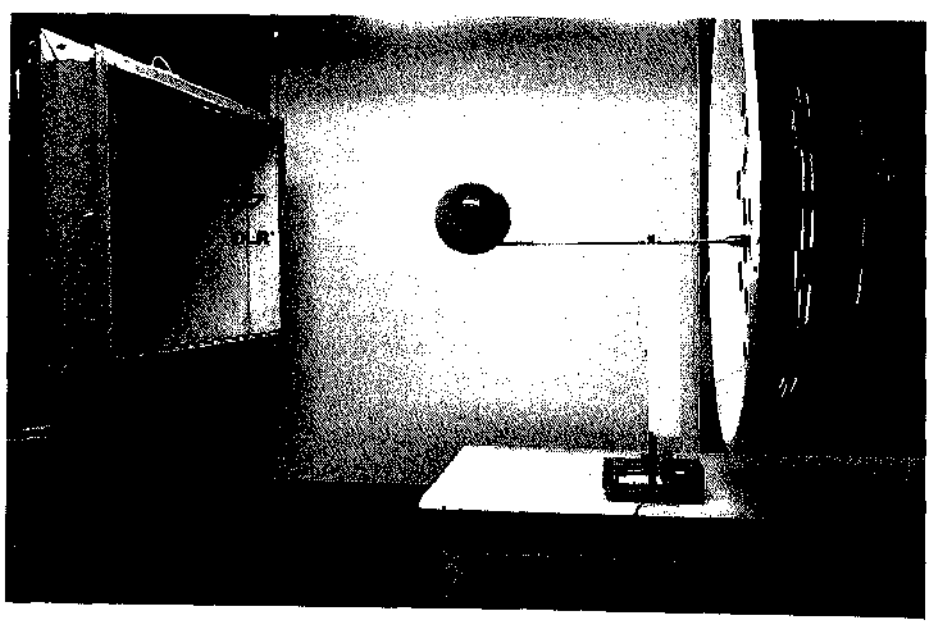

Fig. I. A photograph of the model and the support system

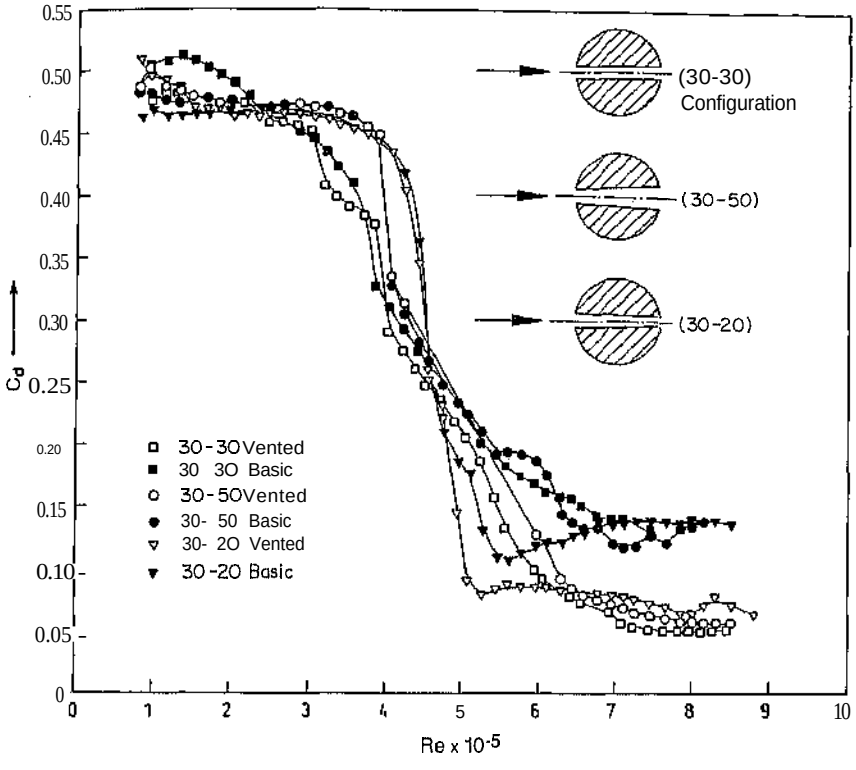

Fig. 2. Variation of net drag coefficient with Reynolds number

Argon laser source from Spectra Physics (SPECTRA-PHYSICS Gmbh, Biiro Mettmann, Aufdem Hüls 16, 40822 Mettmann). The visualization was recorded on a video tape.

3 Results and discussion

3.1 Force measurements - free transition

Figure 2 shows the variation of the net drag coefficient C_d (based on the frontal area of the basic sphere) with *Re.* There is little change of drag at subcritical *Re.* Boundary layer transition seems to occur at much the same *Re* whether the sphere is vented or not. In the supercritical range of *Re,* a significant drag reduction of the order of 50% to 60% is observed. Drag reduction observed seems to be practically independent of the configuration, with the (30-30) showing the highest reduction of about 60%. Data on the basic spheres were obtained by closing the vents of the corresponding spheres. Significant differences, apparently due to inaccuracies in the model fabrication can be noted by comparing the basic configurations. However, a significant change in the nature of the drag curve beyond the critical *Re* is notable. A comparison between the present drag curves and the standard drag curve (Clift et al. 1978) is not meaningful since the measurements referred to in the latter curve are all for spheres with symmetric supports or from free-flight tests. As shown by Raithby and Eckert (1968), the support position plays a very important role beyond the critical *Re.*

The vented area in the present case is 2.25% of the frontal area of the sphere. Experiments were made by reducing the vent area to 1% of the frontal area (by reducing the hole size to 20 mm) using a parallel internal tube. Additionally, a venturi was also placed in the internal flow. Identical drag reduction of the order of 60% was measured in all the cases.

In all the three vented sphere configurations, a stagnation ring occurred close to the entrance on the external surface. This resulted in local separation around the sharp edge of the entrance. It is likely that any effect due to the geometry of the vent was partially affected by the local flow separation.

3.2 Sensitivity of drag reduction

Figure 3 shows the sensitivity of drag reduction to various disturbances. A small piece of an adhesive tape (15 x 4 x 0.2 mm) fixed on the external surface of the vented sphere at about 70° from the centre causes a large offset of the drag reduction. There is however, a 30% drag reduction when compared with that of the basic sphere under same conditions. With two symmetric disturbances, the vented sphere shows higher drag than that of the basic under same conditions. With six such distrubances the drag reduction totally vanishes and the critical *Re* is

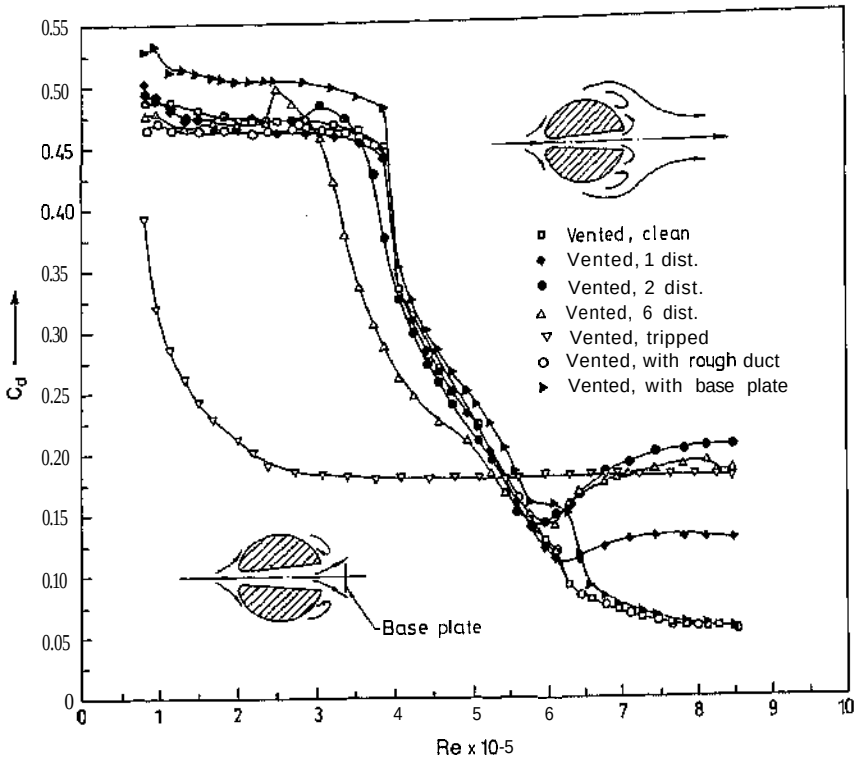

Fig. 3. Sensitivity of drag reduction to disturbances

advanced. With a tripping wire of 1.2 mm diameter placed at 70° from the centerline, there is no change of drag due to ventilation, as compared to the basic sphere under identical conditions.

Whereas the reduction shows large sensitivity to the quality of the external surface, it is relatively insensitive to disturbances in the internal flow. When the smooth internal duct is replaced by a rough one, or when the internal flow is partially blocked by a base plate, there is no change in the drag reduction at a supercritical *Re*. At a subcritical *Re*, the base plate cause higher drag.

3.3 Oil-flow visualization

In the entire range of *Re* tested, i.e., 62500 to 850000, there was no significant change in the point of separation caused due to venting. Laminar separation (L1) alone at about 81° was observed till a *Re* of 160000. At higher *Re*, a turbulent reattachment line (L2) occurred at 99°. As the critical *Re* (defined as *Re* at which $c_d = 0.3$) was reached, the streamwise extent of the bubble was reduced and the turbulent separation line (L3) was asymmetric. At *Re* slightly higher than the critical, both L1 and L2 showed a marked downstream shift. At *Re* of 480000, L1 and L2 occurred at 105° and 120° respectively, with L3 around 145°, as shown in Fig. 4. A clear laminar separation bubble from 105° to 120° was noticed on the range of *Re* tested above 460000. These locations of L1, L2 and L3 are in general agreement with those of Taneda (1978) but

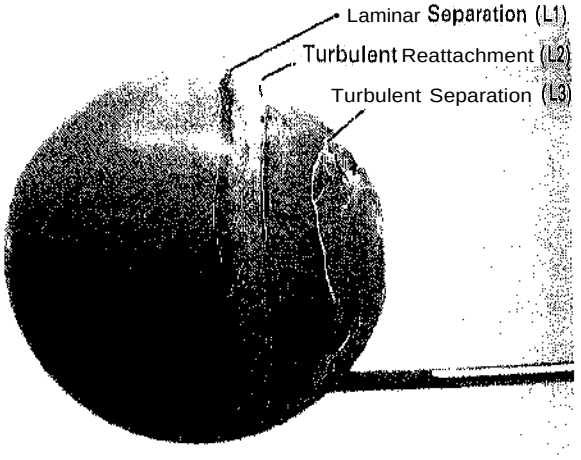

Fig. 4. Oil-flow visualization on (30 50) vented sphere at $Re = 4.6 \times 10^5$

show difference with those of Aachenbach (1972). It is notable that despite the occurrence of a significant drag reduction, the surface (low visualization does not indicate a large change of turbulent separation line due to venting,

Figure 5a shows the oil-flow pattern obtained at *Red* 592000 on the (30-50) vented sphere when a single asymmetric obstacle to the external flow was introduced as explained in 3.2 above. It is seen that aerodynamic disturbances arising from the obstacle break through the laminar separation bubble causing an earlier separation. Simultaneously, a pair of counter-rotating streamwise

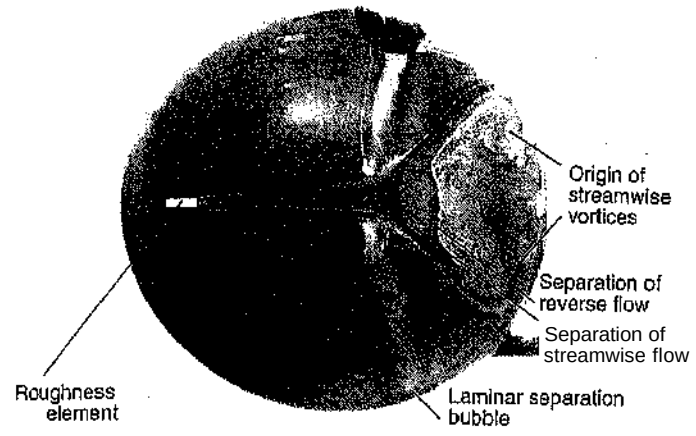

(a)

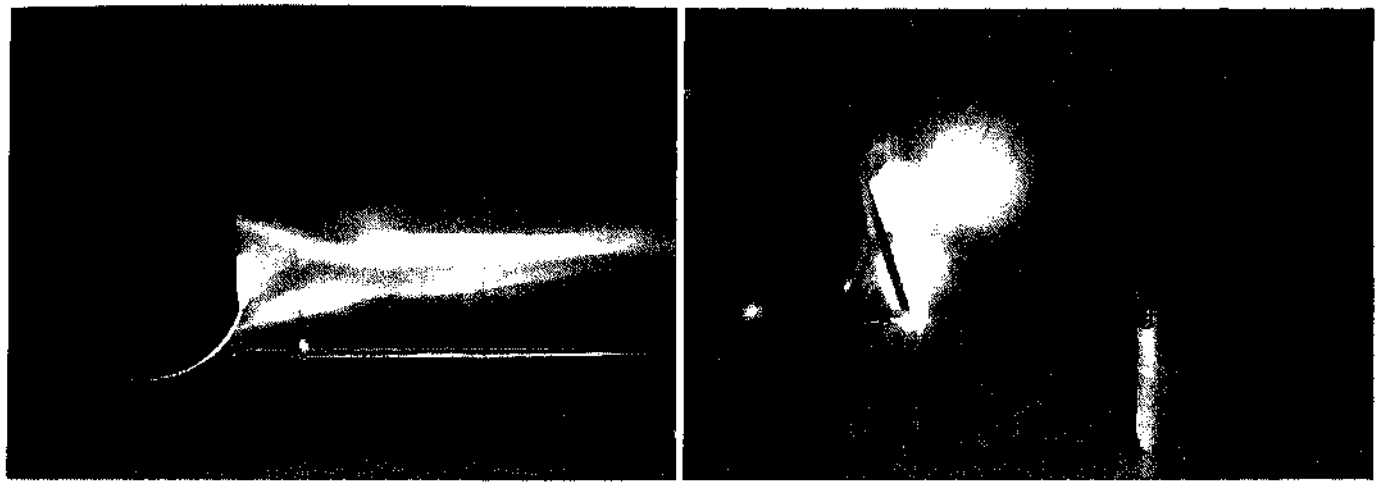

(b)

Fig. 5. a and b. Partial destruction of the base vortex-ring due to a roughness element; a oil flow visualisation at $Re = 5.9 \times 10^5$ b smoke flow visualisation

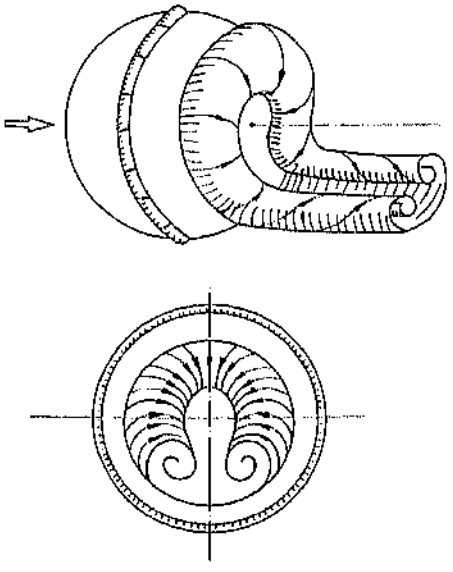

Fig. 6. Schematic of the vortex structure behind a sphere at high *Re* (Taneda, JFM vol. 85, Part-1, 1978)

vortices are discharged from specific locations on the surface. When the experiment was repeated with the vents closed (to correspond to the basic sphere), the laminar separation bubble was locally broken, but there was no specific flow pattern visible at the rear. Two obstacles symmetrically placed about the center of the vented sphere caused two pairs of streamwise vortices and three obstacles (sufficiently displaced) caused three pairs of streamwise vortices. Separation of the streamwise flow and the reverse flow are clearly indicated in Fig. 5(a). With a tripping wire, there were no specific patterns and the separation bubble vanished. There was absolutely no change in the position of the separation line with or without venting.

According to Taneda (1978), the wake behind a sphere at high *Re* is asymmetric and comprises a horseshoe like structure with a pair of counter-rotating streamwise vortices (Fig. 6). The entire structure rotates randomly about a streamwise axis. As a consequence, the sphere at high *Re* always generates a side force whose direction varies randomly. Dallmann and Schewe (1987) have explained the structure of the flow based on topological considerations of three-dimensional separated flows.

3.4 Smoke-flow visualization using laser light sheet

Figure 7 shows typical views (video-prints) seen by the video camera when the laser light sheet is along a vertical

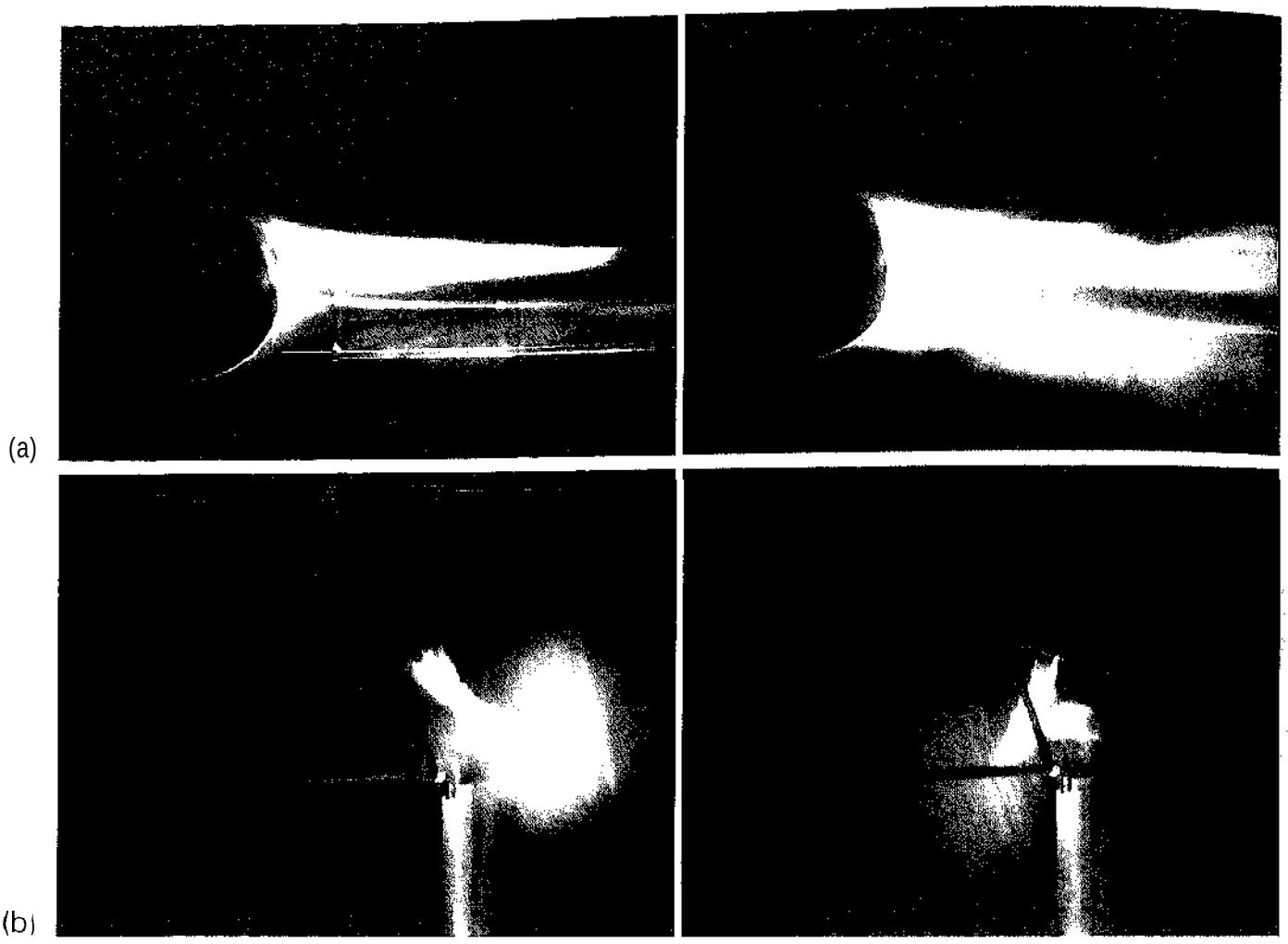

Fig. 7. a and b. Unsteady structure of the wake at high *Re;* a light sheet along the flow direction; b light sheet normal to flow direction at two diameters behind the base

plane in the flow direction and also when it is normal to the flow direction at two diameters behind the base. Views seen in the former setting indicate that the width of the wake is constantly changing. The observed stem-tree structure in the latter setting can interpreted on the basis of the vortical structure of the wake as follows:

The counter-rotating streamwise vortex pair induces a normal component of velocity in the outer or potential flow and this appears as a tree. As the particles are swept away in the streamwise direction, only the incoming flow is visible. Since the entire structure is unsteady and oscillates about a streamwise axis, the stem-tree structure also rotates with the stem always occurring normal to the tree structure. The observations show the extent of oscillation to be 360° whereas Taneda (1978) reports a rotational extent of 180°. Identical structures were observed at several streamwise stations normal to the flow behind the base.

A significant reduction of wake width as a result of venting at supercritical *Re* was noticed in the smoke screen when the light sheet was placed along the flow direction, The vent flow appears to break through the near wake and emerges from the center, thereby splitting the wake. Figure 8 shows typical views as seen by the camera when the sphere has been vented, The view seen with the light sheet normal to the flow direction remains practically unchanged, indicating that the wake has been stabilized. Similar sectional views normal to the flow behind base at several streamwise stations indicated identical patterns.

Flow around the vented sphere seems to attain a stable configuration as shown in Fig. 9. The separated turbulent shear layer is drawn towards the centerline by a counter-rotating vortex ring formed by the vent flow. Consequently, the wake is split by vent flow which breaks through the dead water region. Wake closure is then determined by a ring type singularity.

The sphere is thus aerodynamically streamlined. As a result of capture of the external shear layer towards the center, a significant base pressure increase may be expected. As a result of symmetrisation, the unsteady aerodynamic forces are also reduced.

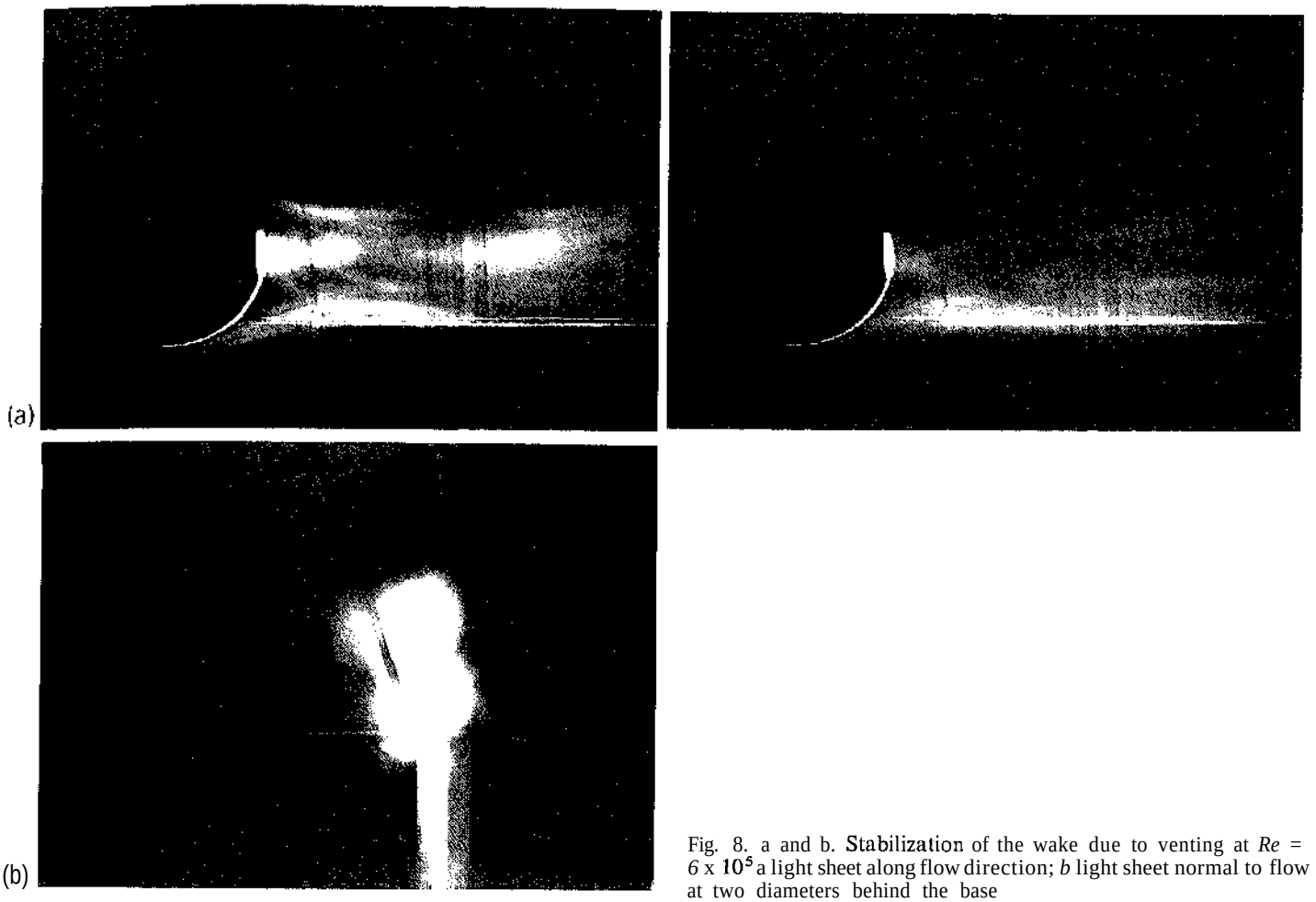

Fig. 8. a and b. Stabilization of the wake due to venting at $Re = 6 \times 10^5$ a light sheet along flow direction; *b* light sheet normal to flow at two diameters behind the base

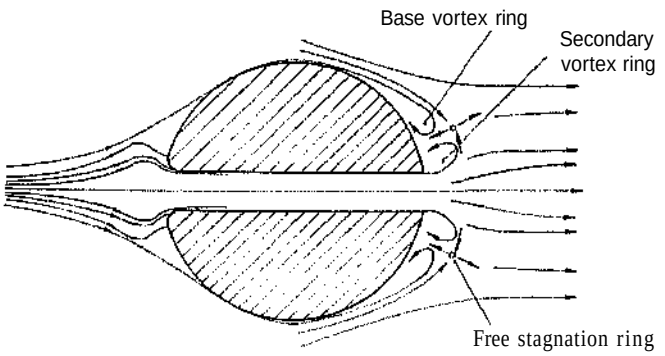

Fig. 9. Schematic of the flow around the vented sphere at $Re = 6 \times 10^5$

As a result of streamlining of the base, the dynamic pressure downstream of the base and consequently the drag due to the support system would be higher for the vented sphere as compared to the basic. Since identical correction factors were used for both the vented and basic spheres, the reported reduction of 50-60% is an underestimate.

Presence of an obstacle destroys the base vortex ring (Fig. 5b) and the flow field is made asymmetric. It is somewhat similar to that of the basic sphere, with the difference that the structure does not oscillate. The views recorded by the camera (Fig. 5b) clearly show the asymmetry of the wake. The stem-tree structure seen with the basic sphere recurs, but the structure is steady and the wake does not rotate.

3.5 Flow visualization in water tunnel

Video prints of the flow visualization in the water tunnel are shown in Fig. 10 at two instances within one period of roll up of the external shear layer at a *Re* of 1800. The internal flow emerges as a jet and travels a certain distance into the wake and is then brought to rest by the reverse flow of the near wake. Particles colouring the edge of the vent flow travel from the base to this stagnation point, deflect asymmetrically and travel upstream towards the separation line of the external flow. Even though all the vent mass was introduced at the center, very little or no mass flow gets out of the near wake from its center.

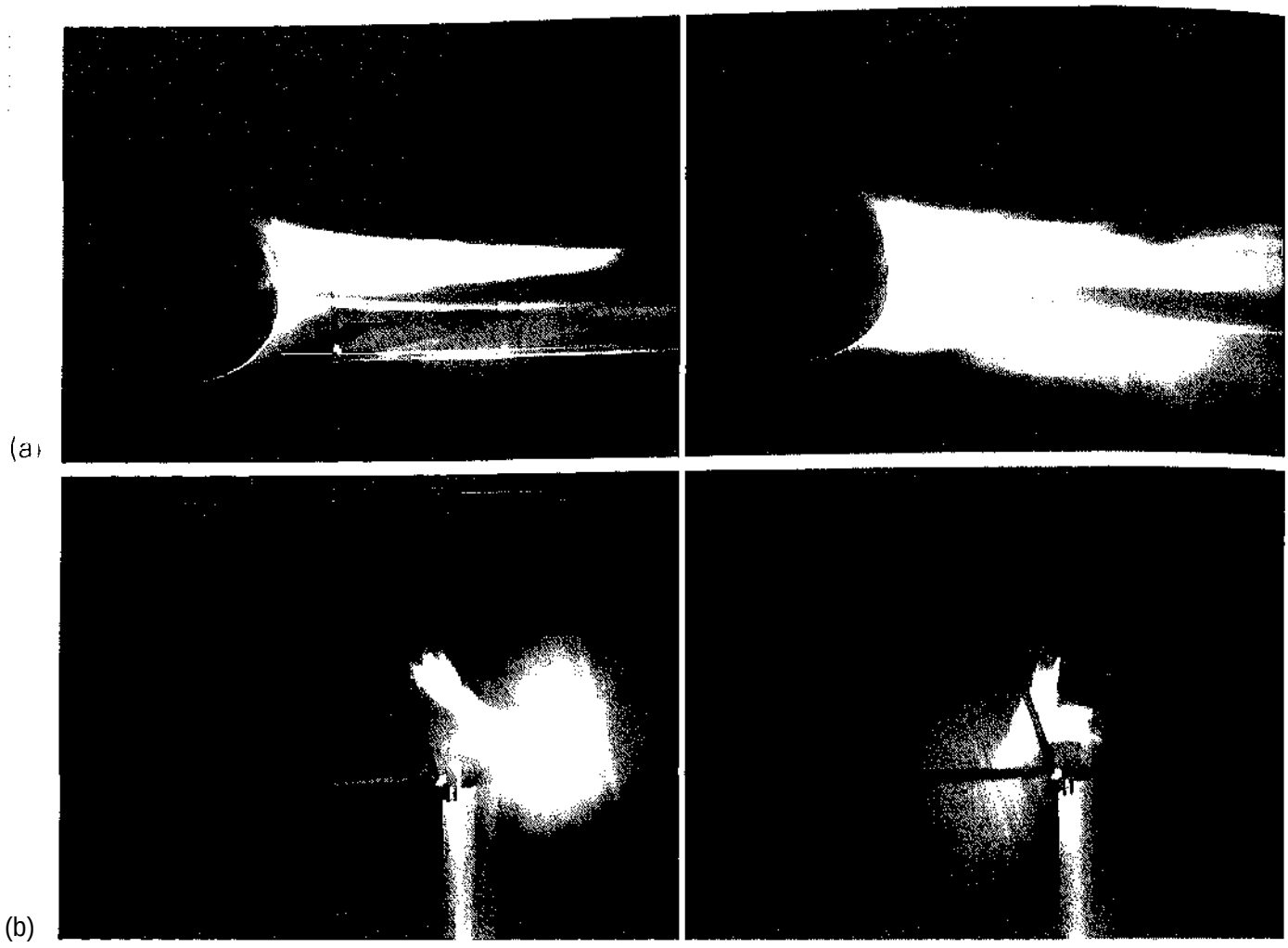

Fig. 7. a and b. Unsteady structure of the wake at high *Re;* a light sheet along the flow direction; b light sheet normal to flow direction at two diameters behind the base

plane in the flow direction and also when it is normal to the flow direction at two diameters behind the base. Views seen in the former setting indicate that the width of the wake is constantly changing. The observed stem-tree structure in the latter setting can interpreted on the basis of the vortical structure of the wake as follows:

The counter-rotating streamwise vortex pair induces a normal component of velocity in the outer or potential flow and this appears as a tree. As the particles are swept away in the streamwise direction, only the incoming flow is visible. Since the entire structure is unsteady and oscillates about a streamwise axis, the stem-tree structure also rotates with the stem always occurring normal to the tree structure. The observations show the extent of oscillation to be 360° whereas Taneda (1978) reports a rotational extent of 180°. Identical structures were observed at several streamwise stations normal to the flow behind the base.

A significant reduction of wake width as a result of venting at supercritical *Re* was noticed in the smoke screen when the light sheet was placed along the flow direction. The vent flow appears to break through the near wake and emerges from the center, thereby splitting the wake, Figure 8 shows typical views as seen by the camera when the sphere has been vented. The view seen with the light sheet normal to the flow direction remains practically unchanged, indicating that the wake has been stabilized. Similar sectional views normal lo the flow behind base at several streamwise stations indicated identical patterns,

Flow around the vented sphere seems to attain a stable configuration as shown in Fig. 9, The separated turbulent shear layer is drawn towards the centerline by a counter-rotating vortex ring formed by (he vent flow. Consequently, the wake is split by vent flow which breaks through the dead water region. Wake closure is then determined by a ring type singularity.

The sphere is thus aerodynamically streamlined, As a result of capture of the external shear layer towards the center, a significant base pressure increase may be expected. As a result of symmetrisation, the unsteady aerodynamic forces arc also reduced.

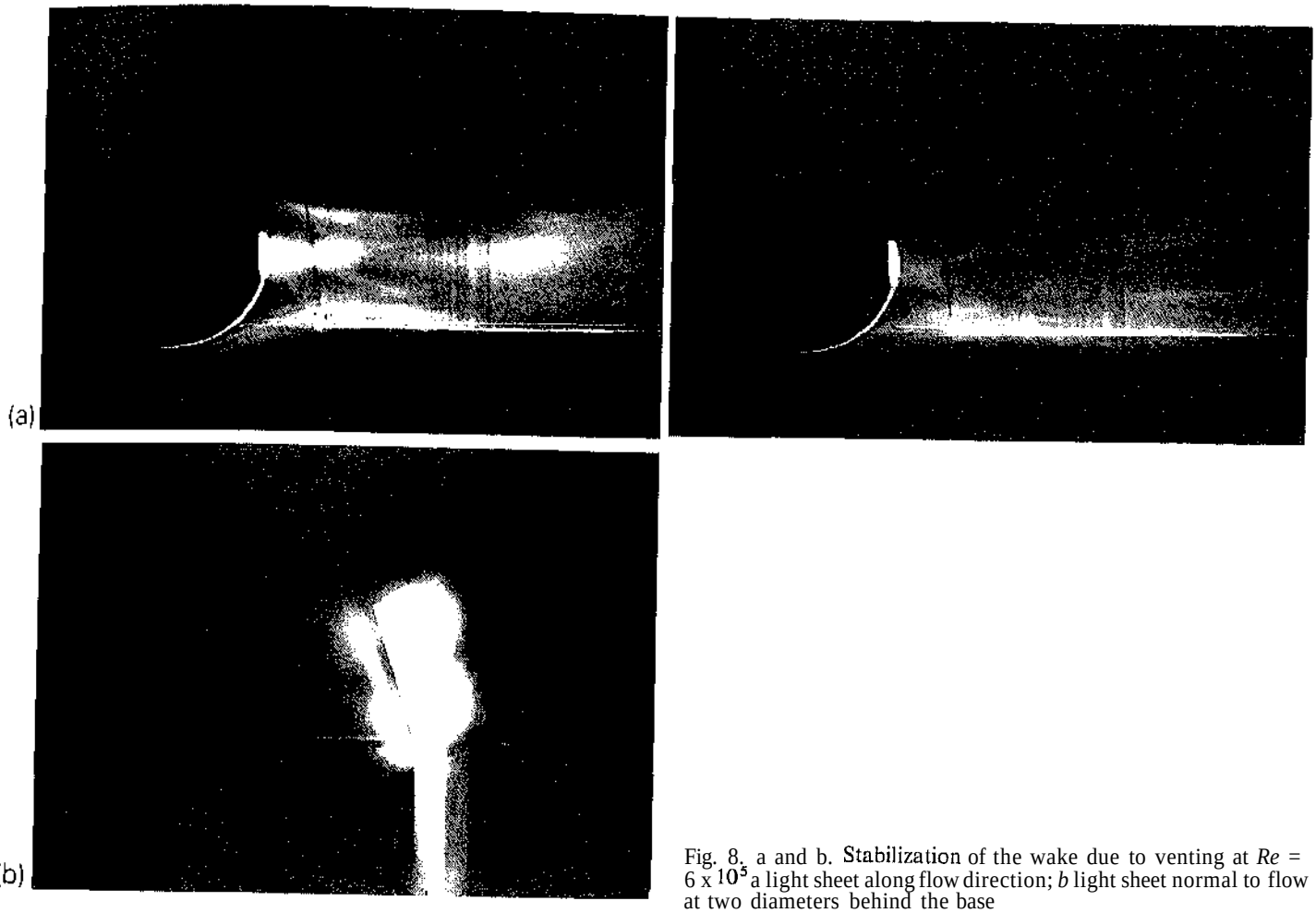

Fig. 8. a and b. Stabilization of the wake due to venting at $Re = 6 \times 10^5$ a light sheet along flow direction; *b* light sheet normal to flow at two diameters behind the base

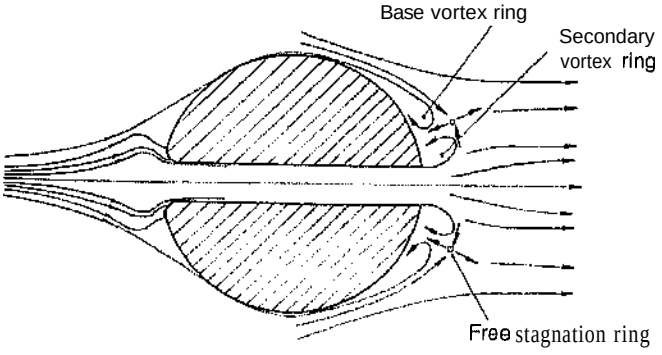

Fig. 9. Schematic of the flow around the vented sphere at $Re = 6 \times 10^5$

As a result of streamlining of the base, the dynamic pressure downstream of the base and consequently the drag due to the support system would be higher for the vented sphere as compared to the basic. Since identical correction factors were used for both the vented and basic spheres, the reported reduction of 50-60% is an underestimate.

Presence of an obstacle destroys the base vortex ring (Fig. 5b) and the flow field is made asymmetric. It is somewhat similar to that of the basic sphere, with the difference that the structure does not oscillate. The views recorded by the camera (Fig. 5b) clearly show the asymmetry of the wake. The stem-tree structure seen with the basic sphere recurs, but the structure is steady and the wake does not rotate.

3.5 Flow visualization in water tunnel

Video prints of the flow visualization in the water tunnel are shown in Fig. 10 at two instances within one period of roll up of the external shear layer at a *Re* of 1800. The internal flow emerges as a jet and travels a certain distance into the wake and is then brought to rest by the reverse flow of the near wake. Particles colouring the edge of the vent flow travel from the base to this stagnation point, deflect asymmetrically and travel upstream towards the separation line of the external flow. Even though all the vent mass was introduced at the center, very little or no mass flow gets out of the near wake from its center.

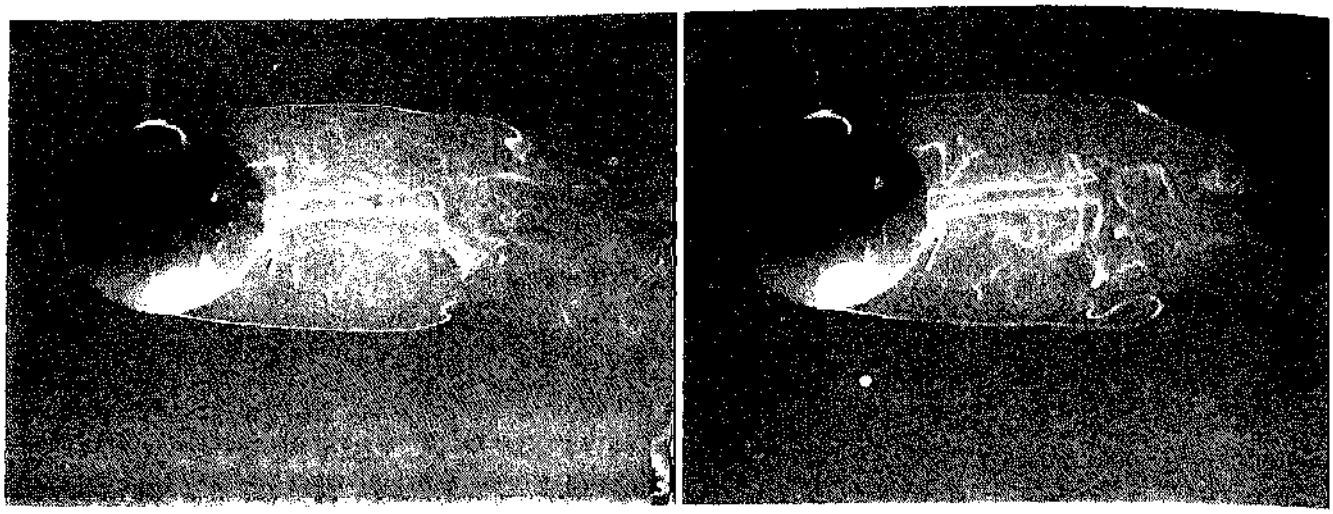

Fig. 10. Flow behind vented sphere at *Re* = 1800 in water tunnel

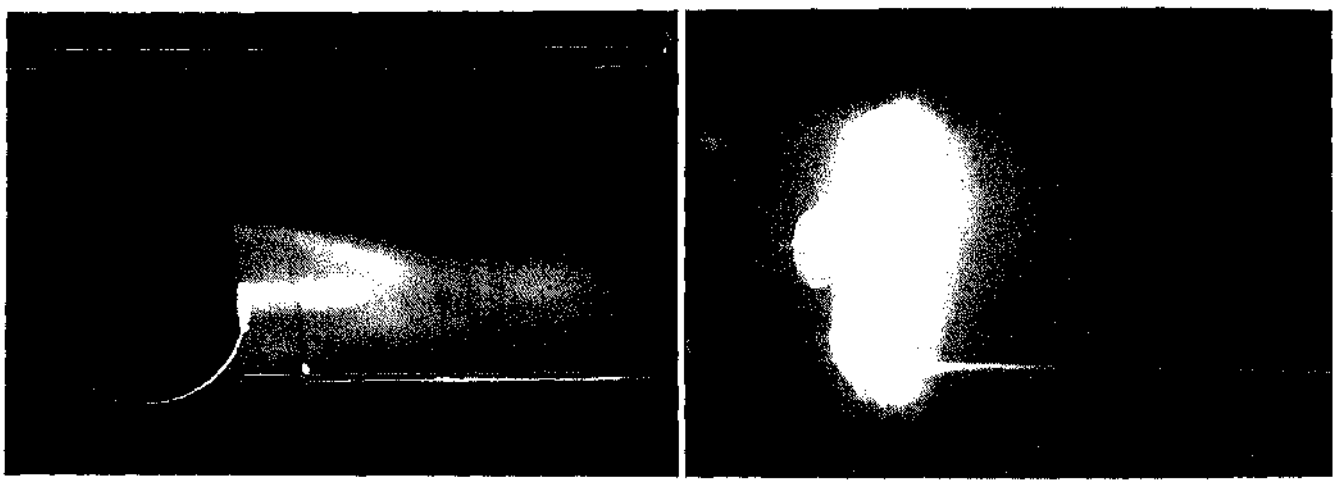

Fig. 11. Stagnation of vent-flow due to tripped boundary layer on vented sphere at $Re = 5 \times 10^5$

As the *Re is* increased, the edge of the internal shear layer becomes turbulent and the length of the internal jet seems to reduce. The internal jet pulsates, deflects and rotates in response to vortex shedding of the external shear layer, but all the same, a clear correlation between the external roll up and the internal flow deflection was not visible.

3.6 Visualization of the effect of tripping the boundary layer

When the external flow on the vented sphere is tripped using a 1.2 mm diameter wire at 60° from the center, the internal jet appears to stagnate inside the near wake (Fig. 11), similar to that at a subcritical *Re*. It appears that the effect of entrainment of the external flow by the jet flow is largely offset. The width of the wake is considerably increased, leading to higher drag. The separation point moves upstream.

4 Conclusions

The drag of a sphere at high *Re* can be reduced to more than half its value by passive ventilation from stagnation region to the base. Simultaneously, (he flow Held around the base is stabilized and made symmetric, leading to reduction of unsteady aerodynamic forces. At high *Re,* the vent flow breaks through the dead water region associated with the near wake and aerodynamically streamlines the base, The streamlining is clone by virtue of a base-vortex-ring beyond the point of turbulent boundary layer separation.

Smoke flow visualized on a laser light screen placed at two diameters behind the base of the sphere shows the

effectiveness of the method in suppressing the flow oscillations.

The drag reduction achieved is very sensitive to the quality of the external surface and relatively insensitive to disturbances in the internal flow. Surface roughness or boundary layer tripping wire on the external flow can completely offset the benefit obtained.

Acknowledgements

The above work was done at DLR in Goettingen, Germany, under a grant from the German Academic Exchange Service (DAAD), Bonn. The first author wishes to thank the Director of DAAD for the grant. Thanks are also due to Dr. F. R. Grosche, Head of the Boundary Layer group at DLR who supported this work with great interest. The authors also wish to thank the technicians Mr. Voss, Mr. Hartmut Mattner and Mr. Detlef Huebner for help during the work. The assistance of Mr. Hartmut Denecke is also acknowledged with thanks.

References

Aachenbach, E. 1972: Experiments on the flow past spheres at very high Reynolds numbers. J. Fluid Mech. 62, 209-221

Bearman, P. W. 1967: The effect of base bleed on the flow behind a two-dimensional model with a blunt trailing edge. The Aeronautical Quarterly, 207–224

Clift, R.; Grace, J. R.; Weber, M. E. 1978: Bubbles, drops and particles. London: Academic Press

Dallmann, U.; Schewe, G. 1987: On topological changes of separating flow structures at transition Reynolds numbers. AIAA 87-1266

Gad-El-Hak, M.; Bushnell, D. M. 1991: Separation control: review. J. Fluids Eng. 5-29

Lin, J. C. et al. 1990: Comparative study of control techniques for two-dimensional low-speed turbulent boundary layer separation. IUTAM Symposium on separated flows and jets, Novosibirsk, USSR

Mair. W. A. 1978: Drag reduction techniques for axisymmetric bluff-bodies. Aerodynamic drag mechanisms of bluff-bodies and road vehicles, pp 161-187. New York: Plenum Press.

Meier, G. E. A.; Suryanarayana G. K.; Pauer H. 1990: Widerstandsverminderung durch Ventilation, pp 311-315. DGLR Bericht 90-06

Raithby, G. D.; Eckert, E. R. G. 1968: The effect of support position and turbulence intensity on the flow near the surface of a sphere, Wärme und Stoffübertragung, Bd1, Heft 2, 87-94

Roshko, A. 1954: On the drag and shedding frequency of two-dimensional bluff-bodies. NACA TN 3169

Suryanarayana, G. K.; Pauer, H.; Meier, G. E. A. 1992: Passive control of the wake of a sphere by Ventilation. IUTAM Symposium on Bluff-Body Wakes, Dynamics and Instabilities, Goettingen, Germany, Springer-Verlag, Berlin, 93-96

Taneda, S. 1978: Visual observations of the flow past a sphere at Reynolds numbers between 10^4 and 10^6. J. Fluid Mech 85, 178-192

Wong, H. Y. 1985: Wake Flow Stabilization by the Action of Base Bleed. Journal of Fluids Eng. Transactions of the ASME, Vol.107,378-384

Wood, C. J. 1964: The effect of base bleed on periodic wake. J. Royal Aeronautical Society, Vol. 68, 477-482